Available online at www.sciencedirect.com
ScienceDirect
Journal of Magnetic Resonance 191 (2008) 239–247
JMR Journal of Magnetic Resonance
www.elsevier.com/locate/jmr

Restricted diffusion and exchange of water in porous media: Average structure determination and size distribution resolved from the effect of local field gradients on the proton NMR spectrum

Jean-François Kuntz [a], Pascal Palmas [a,*], Vincent Level [a], Daniel Canet [b]

[a] *Commissariat à l'Energie Atomique, Laboratory of Physical Chemistry, Le Ripault BP 16, 37260 Monts (Tours), France*
[b] *Nancy-Université, Méthodologie RMN, UMR 7565 CNRS-UHP, Faculté des sciences et techniques, BP 239, 54506 Vandoeuvre-lès-Nancy Cedex, France*

Received 10 October 2007; revised 12 December 2007
Available online 8 January 2008

Abstract

NMR Pulsed field gradient measurements of the restrained diffusion of confined fluids constitute an efficient method to probe the local geometry in porous media. In most practical cases, the diffusion decay, when limited to its principal part, can be considered as Gaussian leading to an apparent diffusion coefficient. The evolution of the latter as a function of the diffusion interval yields average information on the surface/volume ratio of porosities and on the tortuosity of the network. In this paper, we investigate porous model systems of packed spheres (polystyrene and glass) with known mean diameter and polydispersity, and, in addition, a real porous polystyrene material. Applying an Inverse Laplace Transformation in the second dimension reveals an evolution of the apparent diffusion coefficient as a function of the resonance frequency. This evolution is related to a similar evolution of the transverse relaxation time T_2. These results clearly show that each resonance frequency in the water proton spectrum corresponds to a particular magnetic environment produced by a given pore geometry in the porous media. This is due to the presence of local field gradients induced by magnetic susceptibility differences at the liquid/solid interface and to slow exchange rates between different pores as compared to the frequency differences in the spectrum. This interpretation is nicely confirmed by a series of two-dimensional exchange experiments.

Keywords: NMR; Diffusion; Pulsed field gradient experiment; Exchange; Inverse Laplace transform; Size distribution; Internal gradients

1. Introduction

NMR Pulsed field gradient experiments have become an efficient method for investigating the translational displacements of molecular entities bearing nuclear spins, in particular those due to self-diffusion. This is accomplished by probing the self-diffusion phenomenon. When no spatial limits hamper the motion of molecules, free diffusion prevails. Conversely, in a confined structure, the diffusion of fluid molecules is restrained and may reveal the size and shape of the local geometry. This property has been exploited for years in order to characterize the structure of porous media [1]. On the other hand, by using well chosen experimental conditions, the diffusion measurements in a porous structure can lead to the so called "diffusive diffraction phenomenon" [2]. It takes the form of a small oscillation in the *q space* representation (related to the magnetization decay as a function of the area of gradient pulses) showing maxima at q values corresponding to characteristic dimensions of the system. We have recently investigated this effect on model systems of closely packed spheres and on a real porous polymer material. This was done by using different NMR sequences based on classical B_0 gradients (gradient of the static magnetic field) and the alternative approach which uses radiofrequency field B_1 gradients [3]. By selecting different model systems of polystyrene and glass spheres with controlled size and poly-dispersity (size distribution), we specifically investigated the

* Corresponding author. Fax: +33 2 47 34 51 48.
E-mail address: pascal.palmas@cea.fr (P. Palmas).

1090-7807/$ - see front matter © 2008 Elsevier Inc. All rights reserved.
doi:10.1016/j.jmr.2007.12.020

effect of structural disorder and internal magnetic field gradients on the diffraction pattern [4]. When the experimental observation is limited to the main part of magnetization decay, the latter can be considered, to a first approximation, as a simple Gaussian decay. It means that the distribution of molecular displacements can still be considered as Gaussian even in the presence of geometrical restriction. Hence an apparent diffusion coefficient D_{app} can be determined using the Stesjkal and Tanner's equation. The decrease of D_{app} as a function of the diffusion interval (i.e. the time elapsed between the two gradient pulses) can be interpreted in terms of structural characteristics of the porous medium: e.g. the surface/volume ratio S/V at short diffusion intervals and the tortuosity α when a plateau is reached at long diffusion intervals [5–7]. This methodology has been employed here for the model samples of packed spheres of polystyrene and silica glass and for the real porous material already studied by diffusive diffraction [4]. This is now a common approach for obtaining an average information on the porous structure although it does not provide any indication on the structural heterogeneity. The line broadening of the ^{1}H NMR spectrum can have at least two origins: a possible contribution could be a modification of chemical shift due to electrostatic interaction with the polymer, but the main effect certainly results from internal field gradients produced by susceptibility differences at the liquid/solid interface. By using the Inverse Laplace Transform (ILT) of 2D diffusion data obtained with the PFGSTE_BP experiment (Bipolar version of the Pulsed Field Gradient Stimulated Echo Experiment), we show that a distribution of the apparent diffusion coefficient can be resolved in the frequency domain and related to the T_2 relaxation time distribution. These results are confirmed by 2D exchange measurements and correlated to the structural characteristics of the systems showing the relationship between the spreading of resonance frequencies and the distribution of pore geometries.

2. Results and discussion

2.1. Apparent diffusion coefficient as a function of the material average structure

^{1}H NMR spectra of bead samples made of polystyrene and glass silica spheres embedded with water were first recorded using a 5 mm probe for high resolution measurements. A narrow line of about 14 Hz was obtained with polystyrene spheres indicative of a very weak interaction between this material and water and the small magnetic susceptibility difference $\Delta\chi$ at the liquid/solid interface ($\chi = (B/\mu_0 H) - 1$, with B the magnetic induction and H the applied magnetic field). The low value of $\Delta\chi$, in that case is due to the intrinsic properties of both compounds and to the geometrical characteristics of the porous structure made of highly spherical smooth surfaces. On the contrary, with glass spheres, the high value of $\Delta\chi$ between silica and water produces a line of about 2000 Hz width using the same conditions for the sample preparation and NMR experiments. Such a high value of $\Delta\chi$ hampers the measurement of molecular diffusion as it produces local field gradients (denoted g_0 hereafter) which interfere with applied gradients (denoted g hereafter) during the encoding and decoding period of diffusion experiments [3]. In such a situation, the simple STE sequence cannot be used because the major part of the signal is lost and the diffusion pattern is modified due to the cross term gg_0 [8,9]. Hence, diffusion measurements were carried out with the PFGSTE_BP experiment where the influence of local gradients is limited by the use of bipolar gradients pulses separated by a 180° RF pulse instead of a simple gradient pulse [10]. This procedure refocuses the spreading effect of local gradients but does not affect the encoding effect of applied gradient as its polarity is inverted after the 180 pulse. However, this implies that the same local gradient value is felt by nuclear spins during the two gradient pulses. As a consequence the efficiency of the process strongly depends on the scale at which local gradient changes in intensity and direction depending on the porous structure. The evolution of the ratio D_{app}/D_0 (D_0 corresponding to free diffusion at 25 °C) as a function of the diffusion interval Δ are shown in Fig. 1 for the polystyrene and the glass sphere samples. As expected in the context of restricted diffusion, the starting value is less than 1 and decreases for larger diffusion intervals. At long diffusion times the ratio reaches a limit characterizing the tortuosity α defined by

$$\lim_{t\to\infty} \frac{D_{app}(t)}{D_0} = \frac{1}{\alpha} \tag{1}$$

Due to the higher diameter particles, longer diffusion intervals are needed to reach this tortuosity regime in the glass sphere system. The important signal loss due to longitudinal relaxation is responsible for the higher scattering of experimental D_{app} coefficients. At short diffusion intervals, Sen and Mitra [5] showed that the initial decay is directly related to the surface/volume ratio (S/V) of the porosities. We used the mathematical expression of Latour et al. [11] which interpolates between both regimes at short and long diffusion intervals:

$$\frac{D_{app}}{D_0} = 1 - \left(1 - \frac{1}{\alpha}\right) \times \frac{\left(4\sqrt{D_0 t}/9\sqrt{\pi}\right)(S/V) + (1 - 1/\alpha)(D_0 t/D_0\theta)}{(1 - 1/\alpha) + \left(4\sqrt{D_0 t}/9\sqrt{\pi}\right)(S/V) + (1 - 1/\alpha)(D_0 t/D_0\theta)} \tag{2}$$

where θ, a fitting variable, has the dimension of time. Several examples of the determination of the S/V ratio for the pore space of various glass bead packs and rocks using this approach have been published previously [11,12]. We determined, from a fit to experimental data, the parameters S/V, α and θ. A mean particle diameter was evaluated using the expression $d = 6(1/\phi - 1)/(S/V)$ [11]. The different numerical results obtained for both systems of packed spheres are gathered in Table 1 and

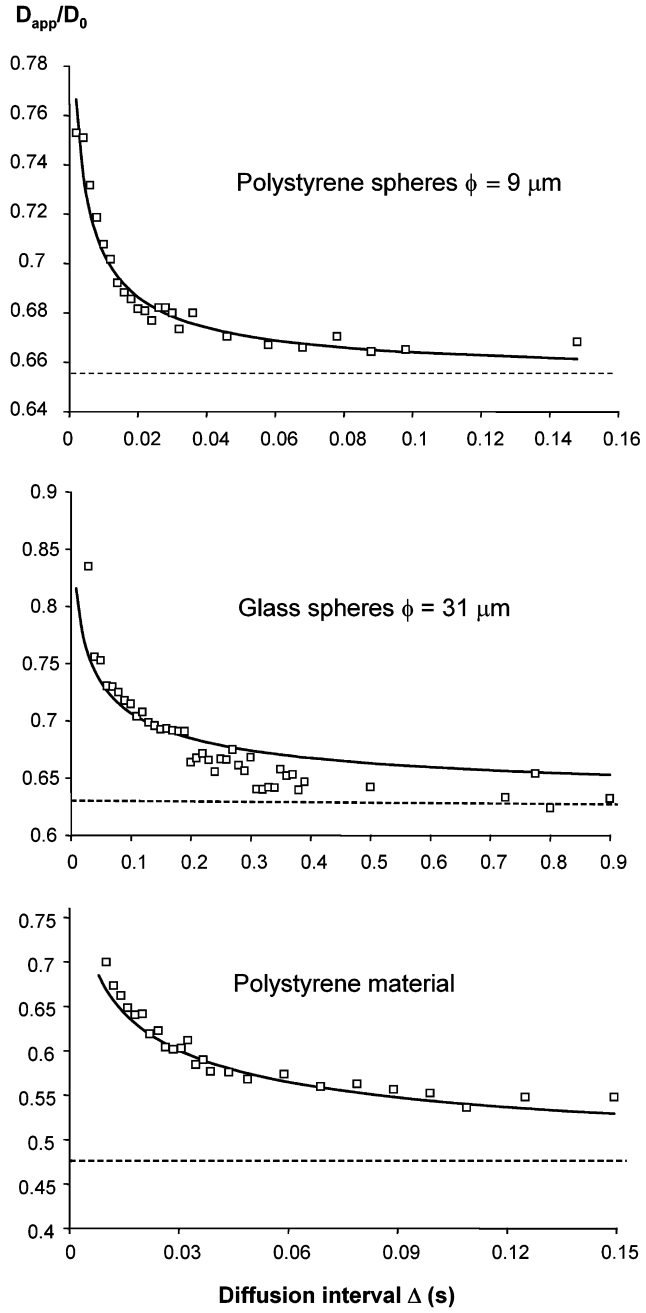

Fig. 1. Evolutions of the ratio D_{app}/D_0 (D_0 corresponding to free diffusion at 25 °C) as a function of the diffusion interval Δ obtained for beads of polystyrene and glass sphere systems and the polystyrene porous material.

show a close agreement with known particle diameters. The tortuosity parameters of 1.5 and 1.6 obtained for the polystyrene and glass spheres are consistent with the theoretical value of 1.61. The latter was calculated using the simple relation $\alpha = 1/(1-\phi)$ with a porosity value $\phi = 0.38$ (where we assumed that the spherical particles adopt, in the cylindrical tube, a closely packed arrangement with a random compactness [11]).

And indeed, applying the same approach to the porous polymer material, the polystyrene di-vinyl benzene (synthesized by inverse emulsion), we obtain a value of 2.1 for α, very close to the value of 2.0 determined by an independent capillarity measurement. Assuming cavities with spherical shapes, we determined a mean pore size of 9.1 μm consistent with SEM images given in reference [3]. However, this result is slightly higher than the value determined from the analysis of the diffusive diffraction pattern obtained by the B_1 gradient method [3]. It has been shown that this is due to the influence of internal gradients which lead, in that case, to an underestimation of D_{app} measured by B_0 gradient experiments.

Table 1
Parameters determined from the analysis of the evolution curve D_{app}/D_0 vs Δ

	Surface/volume ratio S/V (μm^{-1})	Parameter θ (s)	Diameter d (μm)	Tortuosity α
Polystyrene spheres	1.04	0.0043	9.4 (9.1[a])	1.53 (1.61[c])
Glass spheres	0.31	0.16	31.5 (31[a])	1.59 (1.61[c])
Polystyrene porous polymer	0.66	0.052	9.1 (5–15[b])	2.1 (2.0[d])

α, S/V and θ were determined from a fit to experimental data according to the mathematical expression of Latour et al. (Eq. (2)). In parenthesis are given the values (a) determined from laser diffraction measurements; (b) evaluated from SEM images; (c) theoretical; (d) determined from capillary measurements.

2.2. Apparent diffusion coefficient distribution as a function of the structural heterogeneity

A porous material is generally heterogeneous and usually involves a large distribution of pore sizes. Intuitively, each pore may contribute to the total spectrum with a weight proportional to its elementary volume and to the corresponding population. Consequently, the diffusion curve built by taking the total spectrum area is the sum of the different contributions of pores of different sizes. A similar situation occurs for relaxation data, especially T_2 measurements, for which multi-component analysis or Inverse Laplace Transformation (ILT) are well established methods to access the size distribution of pores in different materials [13,14]. More recently, the use of the ILT has been extended in 2 and 3 dimensions producing $T_1/T_2/D$ correlation and exchange data. These methods have provided new possibilities to resolve complex mixtures, for example the separation and quantification of water/oil ratio in rocks, even using low field spectrometers [15–18].

Another consequence of the structural heterogeneity is the spreading of frequencies which mainly results from the distribution of magnetic susceptibility differences at the liquid/solid interface. Thus, each frequency can be assigned to a particular local geometry, provided that the exchange between different sites is sufficiently slow as compared with the frequency differences. We show here that

both effects can be visualized in the same experiment, giving a direct access to individual NMR parameters without the need of any deconvolution. This is remarkably shown in the 2D maps (D vs resonance frequency) of Fig. 2 obtained for the glass spheres system. In the case of polystyrene spheres, the phenomenon was not observed because the linewidth is very small. At a short diffusion interval, $\Delta = 15$ ms, chosen at the beginning of the restricted diffusion regime (see Fig. 1), the two-dimensional correlation peak is clearly tilted revealing a net distribution of apparent diffusion coefficients between $\approx$1300 and $\approx 1600 \times 10^{-12}$ $m^2\ s^{-1}$. The reproducibility of this result was verified paying special attention to the phase stability during the whole diffusion experiment. Moreover, it cannot be a numerical artifact arising from the ILT transform because variations of the diffusion coefficients can also be observed using a classical least squares analysis (with one or two Gaussian components). These results nicely demonstrate that, at short diffusion intervals, the water molecules are more or less confined in different local geometries, each of them producing one D value and one resonance frequency. This leads to a spreading in both dimensions related to the pore size distribution in the material. The smallest pores (denoted A) give rise to the lowest apparent diffusion coefficients. The corresponding NMR signals are relatively weak and located at the more shifted part (at low field) of the spectrum due to the influence of larger local field gradients. When Δ is increased, the confinement is gradually lost and the molecules have time to exchange between different structural environments (cavities). As a consequence, the distribution of diffusion coefficient is gradually damped. At $\Delta = 400$ ms which falls in the tortuosity regime (see Fig. 1), the 2D correlation peak is almost horizontal providing a unique value for D_{app} whatever the resonance frequency. The evolution curves of D_{app} as a function of Δ obtained at three different resonance frequencies of the ^{1}H spectrum are shown in Fig. 3. Although there is a greater dispersion of D_{app} data (because a peak height, measured at a given frequency, is much more noisy than the total spectrum area) different slopes at short Δ can be seen for the three positions A, B and C. From a fit to experimental data we obtain the corresponding sphere diameters $d_A = 26$ μm, $d_B = 38$ μm and $d_C = 61$ μm, which are consistent with the range of particles diameters as measured by Laser Diffraction [4].

The same phenomenon was observed in the porous polymer sample. A superposition of 2D maps obtained with three different values of the diffusion interval Δ is shown in Fig. 4. Again, a distribution of the apparent diffusion coefficient D_{app} is clearly seen at $\Delta = 11$ ms and is gradually damped for increasing Δ values. The range of diffusion coefficients (between $\approx$800 and 1500×10^{-12} $m^2\ s^{-1}$) is larger than in the previous case, and a slight tilt remains even at 500 ms. This confirms the more complex structure of this porous network as compared with the packed sphere system [3,4]. The fit of the evolution of the ratio D_{app}/D_0 vs Δ for two frequencies A and B at both sides of the spectrum (Fig. 5) yields a range of cavity dimensions between 4 μm (B) and 24 μm (A), in agreement with the SEM images of the surface [3]. The distribution of the local geometry as a function of the resonance frequency is also confirmed by T_2 measurements using the CPMG experiment. This is shown in the 2D (frequency, T_2) map presented in Fig. 6 obtained after an Inverse Laplace transform with respect to the evolution time τ in the CPMG experiment. As for diffusion measurements, a strongly tilted correlation peak is obtained revealing a wide T_2 distribution between 3 and 18 ms. In agreement with diffusion experiments, the low field part of the spectrum corresponds to the smaller pores which give rise to the shortest relaxation times.

2.3. Exchange measurements as a function of the structural heterogeneity

To investigate the effect of the structural heterogeneity on the ^{1}H NMR spectrum, another possibility consists in

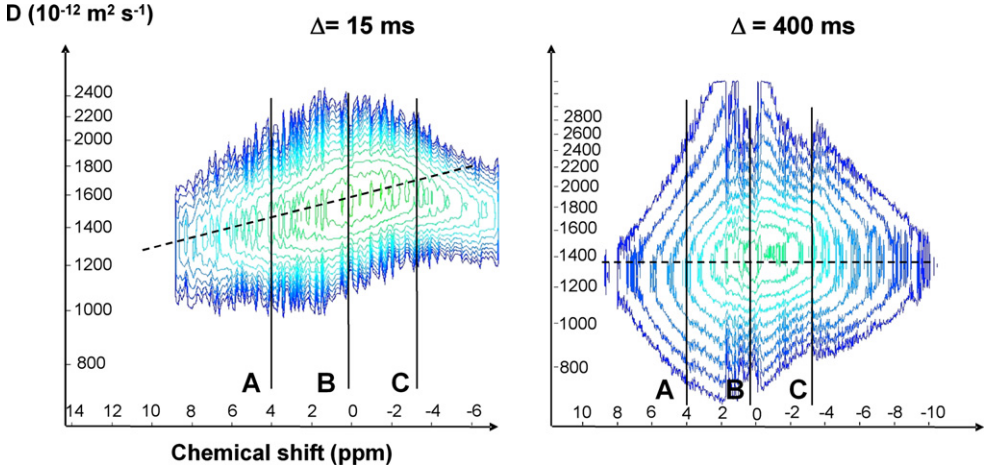

Fig. 2. Two-dimensional maps (resonance frequency, diffusion) obtained on the glass spheres system by Fourier transform of the first dimension (acquisition dimension) and inverse Laplace transform of the second dimension (evolution according to diffusion) for two different diffusion intervals $\Delta = 15$ ms and $\Delta = 400$ ms. The gradient pulse length was $\delta = 2.4$ ms.

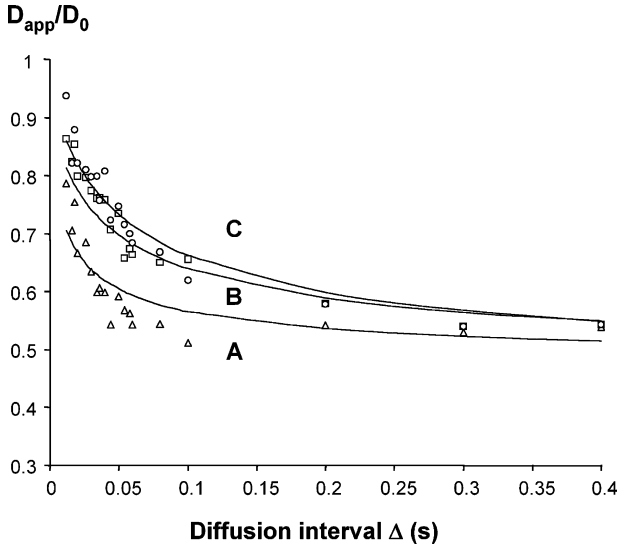

Fig. 3. Evolution of the ratio D_{app}/D_0 as a function of the diffusion interval Δ obtained at 3 different resonance frequencies on the ^{1}H spectrum (denoted A, B and C in Fig. 2).

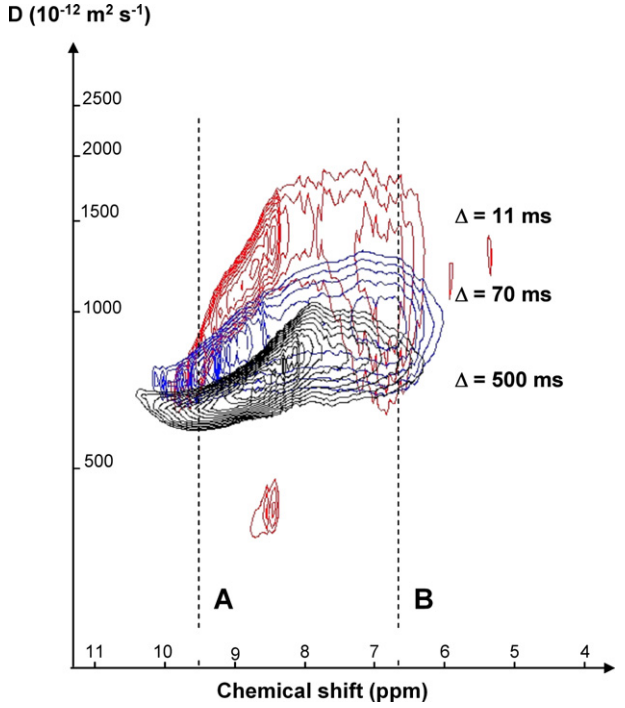

Fig. 4. Superposition of two-dimensional maps (resonance frequency, diffusion) obtained on the polystyrene porous material for three different diffusion intervals $\Delta = 11$ ms and $\Delta = 70$ ms and $\Delta = 500$ ms.

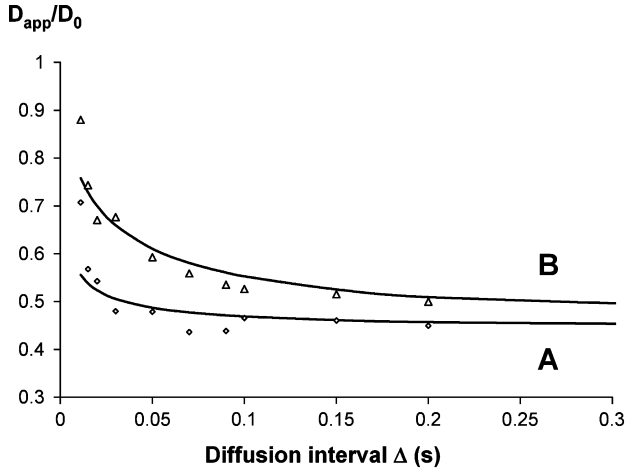

Fig. 5. Evolution of the ratio D_{app}/D_0 as a function of the diffusion interval Δ obtained at 2 different resonance frequencies of the ^{1}H spectrum (denoted by A and B on Fig. 4).

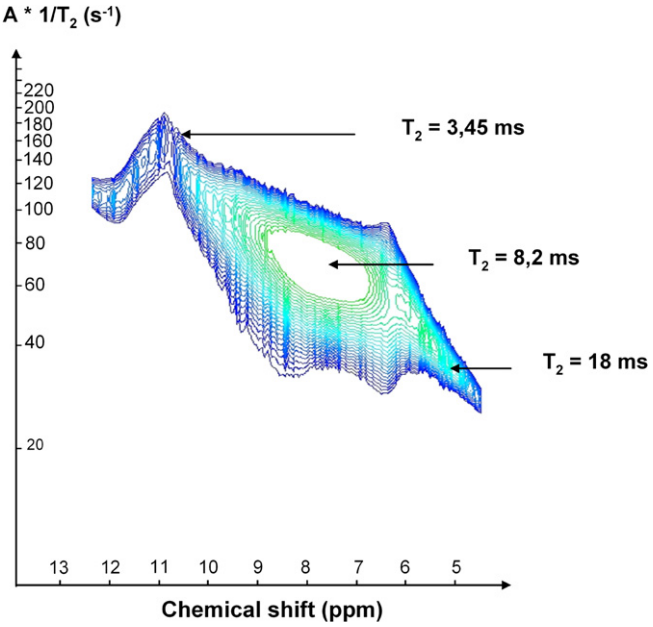

Fig. 6. Two-dimensional map (resonance frequency, T_2 relaxation time) obtained on the polystyrene material by Fourier transform of the first dimension (acquisition dimension) and inverse Laplace transform of the second dimension (evolution according to transverse relaxation) of the CPMG experiment. A is a conversion parameter given by the mathematical expression $A = 1/(\Delta\ \delta^2\gamma^2\ 10^{-10})$ (with $\gamma = 26.75 \times 10^7$ rad T^{-1} s^{-1}). Using arbitrary values $\delta = 1.2$ ms and $\Delta = 0.18$ s for the calculation we obtained $A = 0.54$.

probing possible changes of the environment experienced by individual spins. In early works, Callaghan et al. reported the observation of exchange of water molecules in a porous media using $T_2 - T_2$ correlation and 2D ILT treatment [19]. The two-dimensional EXSY (Exchange Spectroscopy) sequence is also a well known method for monitoring exchange phenomena between different sites [20,21]. It requires the existence of different resonance frequencies for the exchanging sites and a frequency difference $\Delta\nu$ larger than the exchange rate. While this NMR sequence has been widely used to study chemical or conformational exchange processes, its application to the study of a liquid in a porous material has not been really exploited, at least to the best of our knowledge. In a recent work Knagge et al. have reported the use of hyper hyperpolarized Xenon to characterize the pore shape and exchange

phenomena in a porous silicon system [22]. They benefited of the strong sensitivity of Xenon chemical shift toward its structural environment which leads to well separated lines for the different sites. Although this feature does not prevail here (continuous spectrum), we can nevertheless hope to observe exchange phenomena between different regions since the latter are characterized by different chemical shifts produced by different internal gradients.

2.4. Glass sphere system

The exchange data obtained for the crude material with mixing times $t_m = 5$ ms and 1 s are shown in Fig. 7. For mixing times up to 15 ms, the two dimensional peak is almost diagonal. It means that within such a small time interval, the exchange of water molecules between two different structural environments (i.e. two cavities) has a low probability because the mean square displacement $\bar{r}$ of molecules is smaller than the particles size of 31 μm. $\bar{r}$ was estimated to be less than 12 μm for $t_m = 15$ ms. This value was calculated within the assumption of a Gaussian distribution of displacements, using the simple equation $\bar{r} = \sqrt{6D_0 t}$ with $D_0 = 1.9 \times 10^{-9}$ m^2 s^{-1} at 290 K. As t_m is increased, a gradual modification of the two dimensional pattern is observed leading to a more rectangular correlation peak. This result definitely demonstrates that the different parts of the proton spectrum arise from different regions in which molecules can exchange within a time scale of a hundred milliseconds. The superposition of 1D cross sections obtained for different mixing times and taken at a specific frequency $\nu_1 = \nu_R$ in the F_1 dimension is shown in Fig. 8a. The dynamics of exchange can be evaluated from the build-up curves corresponding to six off-diagonal $\nu_2 = \nu_A$ to ν_E and to the diagonal position $\nu_1 = \nu_R$ (Fig. 8b). While the intensity always decreases at the diagonal position R, the intensity increases, reaches a maximum and then decreases as a function of the mixing time at non diagonal positions A–E. The increase is due to the exchange between region R and regions A–E (which involve different geometries) while the decreasing part is essentially governed by T_1 relaxation. Under the assumption of two sites, the intensity of the exchange peak in an EXSY experiment is proportional to the term $\frac{1}{2}[1 + \exp(-2kt_m)]\exp(-t_m R_1)$ for the diagonal peaks and $\frac{1}{2}[1 - \exp(-2kt_m)]\exp(-t_m R_1)$

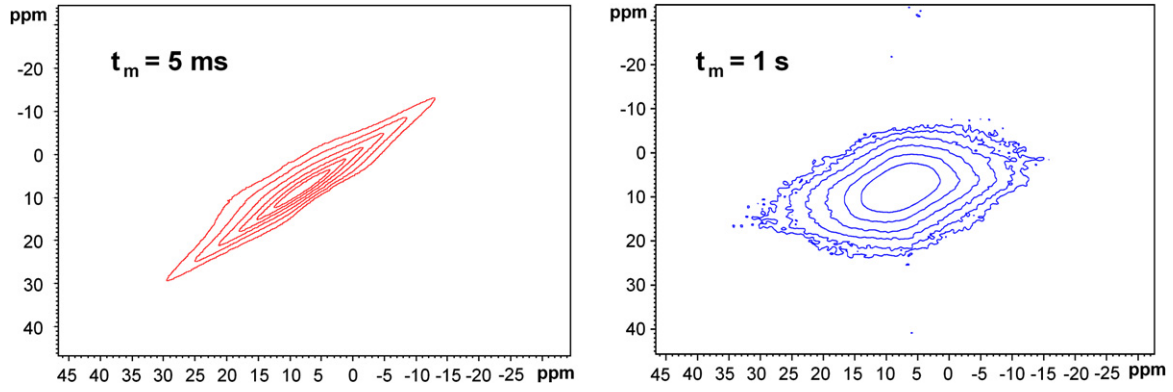

Fig. 7. Two dimensional exchange data of water in the packed glass sphere system (crude fraction) obtained with mixing times $t_m = 5$ ms and 1 s.

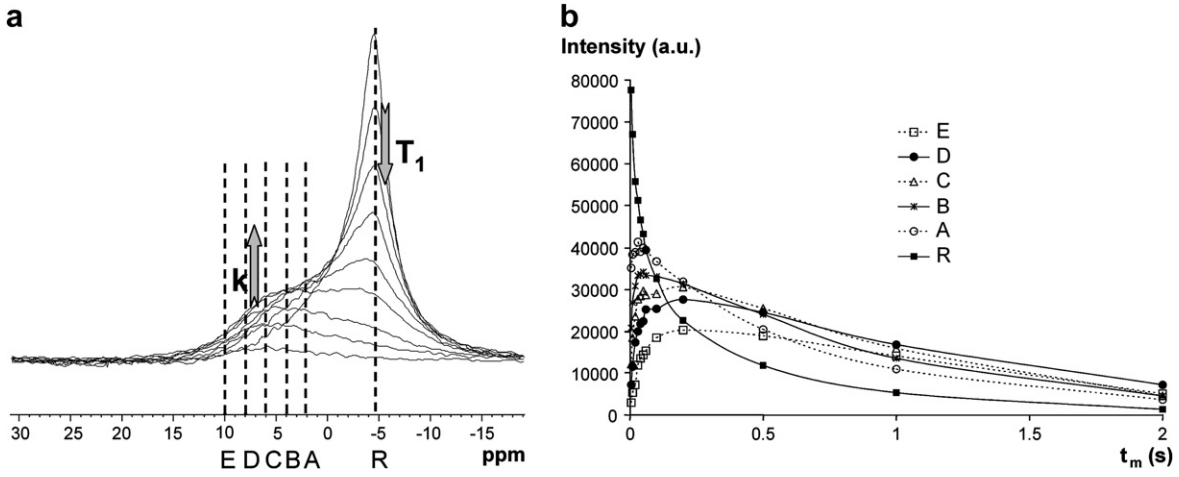

Fig. 8. (a) Superposition of 1D cross sections obtained for the glass sphere system (see Fig. 7) at different mixing times and taken at a specific frequency $\nu_1 = \nu_R$ in the F_1 dimension. The k arrow indicates the effect of exchange whereas the T_1 arrow indicates the effect of longitudinal relaxation. (b) Build-up curves constructed from the intensity measured at six different frequencies $\nu_2 = \nu_A$ to ν_E (off diagonal contribution) and $\nu_1 = \nu_R$ (diagonal contribution). The k arrow indicates signal growth due to exchange whereas the T_1 arrow indicates signal decrease due to longitudinal relaxation.

for the off diagonal peaks, where k is the exchange rate and $R_1 = 1/T_1$ the longitudinal relaxation rate. In the present case, a given site can exchange with a number of other sites of different geometries. Thus, a cross-peak may result from different contributions due to direct or relayed pathways. In such a situation, the relaxation matrix formalism can be used to account for the whole evolution curves. It is however more convenient to limit the data analysis to short mixing times in such a way that any cross-peak can be considered as arising from a unique direct pathway. The intensity variation as a function of t_m is, to a first approximation, linear and given by the simple relation ($I/I_0 \approx k\ t_m$). I_0 is the equilibrium magnetization, an estimation of which is given by the diagonal peak measured at the shortest mixing time. k^{-1} is determined from the initial slope of the build up curves for the crude and sifted fractions of glass spheres. The corresponding values of the mean square displacement were also calculated using the relation given above ($\bar{r} = \sqrt{6D_0 t_m}$) and gathered in Table 2. These results show first that the extent of exchange rates between 3 and 50 Hz is smaller than the differences in resonance frequency of the various sites confirming the slow exchange regime and the inhomogeneous character of the ^{1}H spectrum. Second, the lowest distance which can be determined is similar for both systems and close to the mean radius of the spherical particles. Third, it can be noticed that the mean displacement of water molecules starting from a given magnetic environments (for example R) to reach another magnetic environ-

Table 2
(i) Exchange time constant k^{-1} obtained, for the crude and sifted fractions of glass spheres, by measuring the initial slope of the build up curves for six different chemical shifts $v_2 = v_A$–v_E for a given cross section located at $v_1 = v_R$ (which corresponds to the intensity maximum in the normal 1D spectrum—see Fig. 8

	Crude fraction ($\sigma \approx 30\%$)		Sifted fraction ($\sigma \approx 18\%$)	
	k^{-1} (ms)	d (μm)	k^{-1} (ms)	d (μm)
E	158	46	362	69
D	101	36	125	41
C	48	25	60	28
B	29	20	35	21
A	19	16	20	16

(ii) Corresponding values of the mean square displacement calculated using the relation given in the text.

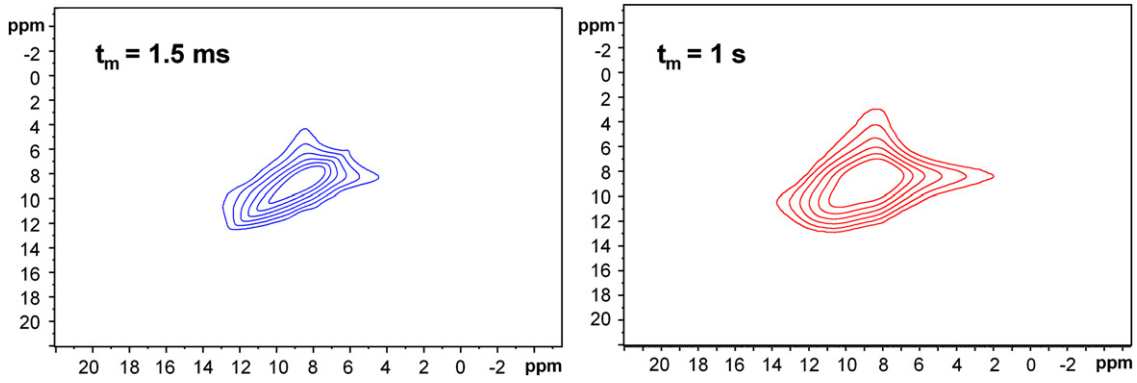

Fig. 9. Two dimensional exchange data of water in the polystyrene porous material obtained for mixing times $t_m = 1.5$ ms and 1 s.

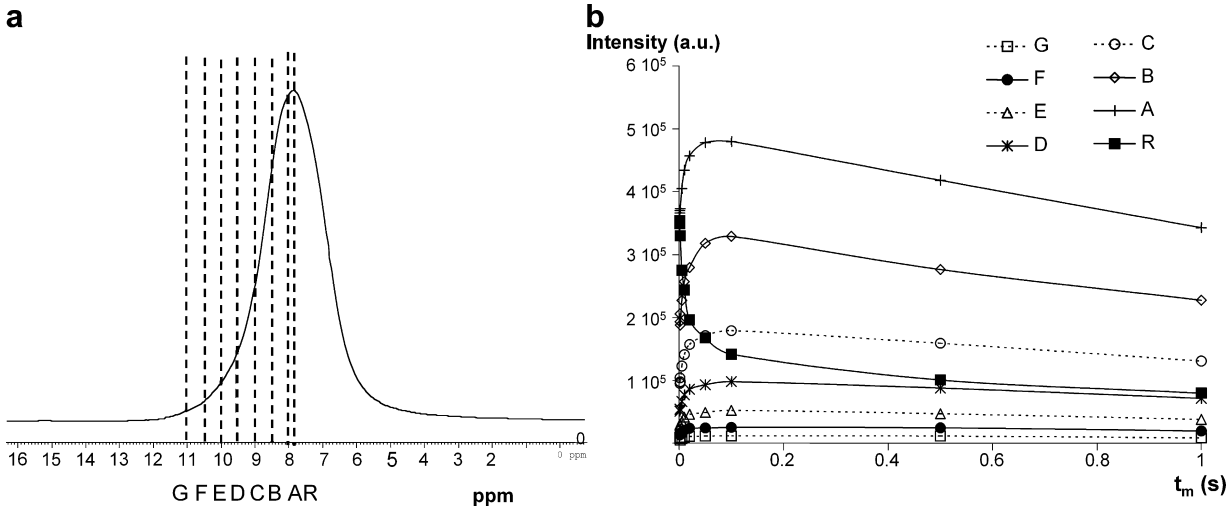

Fig. 10. (a) 1D ^{1}H spectrum obtained on the porous polystyrene material (b) Build-up curves constructed from the intensity measured at seven different frequencies $v_2 = v_A$ to v_G (off-diagonal contribution) and $v_1 = v_R$ (diagonal contribution).

ment (for example A,B...E) is higher in the sifted fraction. This observation is presumably related to the probability of finding two different geometrical environments at a short distance from each other. This probability is expected to be higher in the crude fraction because it is less ordered.

2.5. Polystyrene porous material

Two-dimensional exchange experiments were also performed on the embedded polystyrene porous material. As seen in Fig. 9, the shape of the two-dimensional correlation peak is again function of the mixing time due to an increase of the exchange phenomenon. However, even at the shortest achievable value $t_m = 1.3$ ms (which corresponds to a mean squared displacement of ca. 5 μm), the pattern is not completely diagonal. This result shows, in agreement with diffusion data, that at least a small fraction of the water molecules can move to another geometrical environment within a very short time. It confirms the higher heterogeneity of this system (observed in the SEM images [3]) at the level of the pore size. The build-up curves corresponding to seven different chemical shifts $v_2 = v_A$ to v_G on a given cross section located at $v_1 = v_R$ (which corresponds to the maximum intensity in the normal 1D spectrum) are shown in Fig. 10. Mean square displacements in the range 8–134 μm were determined from the determination of the initial slopes. The lowest distance is again in agreement with the pore dimensions estimated from the SEM images. However, it cannot be directly related to the mean pore-to-pore distance in this material because of the exchange phenomenon seen at short times. The latter could be ascribed to intra-pore displacements.

3. Conclusion

In this paper the restricted diffusion phenomenon has been investigated in different porous media including model systems of calibrated closely packed sphere particles (of polystyrene or glass) and a polystyrene porous material. Using a conventional approach, we were able to determine, for the different samples, average structural parameters (surface/volume ratio and the tortuosity). The use of the Inverse Laplace transform in the second dimension of the diffusion experiment reveals, for short values of the diffusion interval Δ, a clear dependency of the diffusion coefficient as a function of the resonance frequency. This dependency which is gradually damped as Δ increases is shown to be related to the pore size distribution. This is confirmed by the observation of a similar distribution of T_2 relaxation times measured by CPMG. Two-dimensional exchange experiments have been carried out to monitor the exchange dynamics of molecules in these different porous media. A quantitative analysis of the two-dimensional correlation pattern has been used to derive characteristic distances for the exchange phenomena taking place in these systems. These results are consistent with diffusion measurements and are in agreement with the known dimensions and the structural heterogeneity (determined experimentally or theoretically). All these data definitely demonstrate that each resonance frequency in the water proton spectrum corresponds to a particular magnetic environment produced by a given pore geometry in the porous media. This spreading of resonances is due to (i) local field gradients induced by magnetic susceptibility difference at the liquid/solid interface and (ii) exchange between different pores at rates lower than the frequency differences in the spectrum.

4. Experimental section

All experiments were carried at 290 K on a 9.4T Bruker Wide Bore spectrometer (proton resonance frequency of 400.13 MHz) equipped (for diffusion experiments) with a standard Bruker micro2.5 imaging system capable of delivering a maximum gradient strength of 100 G cm^{-1} in each of the three directions. This latter equipment was employed with the z-gradient for diffusion experiments. We used two different bird cage coils (10 mm and 25 in diameter) producing 90° pulses of 10.5 and 21.4 μs, respectively. Diffusion measurements were performed using the 11 intervals PFGSTE_BP sequence [10] in order to minimize T_2 attenuation and background gradient effects due to magnetic susceptibility differences between water and the polymer matrix. The pulsed field gradient length δ was set to values in the range 2–6 ms and the diffusion intervals Δ was varied between 4 and 900 ms. δ was kept constant for the whole series of measurements performed on a given sample with different diffusion intervals Δ. The q space encoding was achieved by incrementing linearly the gradient amplitude between 2% and 95% in 32 steps. The gradient strength was calibrated with water and octanol.

Models systems of packed sphere particles were prepared with calibrated spheres controlled by laser diffraction: (i) polystyrene spheres purchased from Merck S.A. (mean diameter 9.1 μm) with a weak size distribution (dispersion $\sigma \approx 14\%$) (ii) glass spheres provided by Malvern S.A. (31 μm, dispersion $\sigma \approx 30\%$) (iii) a second fraction of glass spheres with less dispersion (31 μm, $\sigma \approx 18\%$) produced by a sifting procedure. The dispersion σ is defined as the ratio, expressed in percentage, of the diameter standard deviation over the mean diameter. As described in reference [4], the spheres were first washed three times and filled with deionised water, then introduced in standard NMR tubes (inner diameter of 9 mm), and centrifuged during 20 min to achieve random loose packing. Porous samples of cross-linked polystyrene were obtained by an inverse phase emulsion process (PolyHipe) using a mixture of styrene and divinylbenzene. An opened porosity of 72% was determined both by Helium picnometry and weighting. The SEM images presented in reference [3] revealed a heterogeneous porous structure with a complex network of more or less spherical cavities with dimensions in the range 5–15 μm and connected by smaller channels. Mercury intrusion porosimetry measurements gave an estimation of their

mean size around 3 micrometers. Cylindrical samples with dimensions ($\phi = 4$ mm, $h = 18$ mm) and ($\phi = 23$ mm $h = 25$ mm) were prepared for 10 mm, and 25 mm NMR sample tubes, respectively. The porous structure was embedded by total immersion in water while maintained at a reduced pressure until the disappearance of air bubbles (about 1 h). After this procedure, the cylinders were systematically dried outside and weighted to control the filling factor before analysis. The samples were then inserted in NMR sample tubes especially reduced in their length and carefully locked with a cap and parafilm in order to minimize the desorption phenomenon. The homogeneity of water concentration through the sample was evaluated by 3D gradient echo imaging. This method being strongly sensitive to magnetic susceptibility differences, any air bubble would appear as characteristic black and light spots in the image. To further control the stability of the system, a 1D spectrum and a standard diffusion experiment were performed at the beginning and at the end of each series of experiments. Thereby, it was seen that a loss of a few percent of the water content had no detectable consequences on NMR results.

The diffusion curves built from the area of the whole spectrum were fitted using a least squared fitting procedure according to the Stesjkal and Tanner's equation [23]. A second minor Gaussian component was also added when necessary to account for the end of the attenuation. However, the values of D_{app} where systematically extracted from the first component corresponding to the initial decay. Two dimensional (frequency, diffusion) maps were generated by applying a Fourier transform in the first dimension and an Inverse Laplace transform in the second dimension. ILT was carried out by using the module MAXENT (entropy maximisation) in the GIFA software [24].

Two-dimensional homonuclear EXSY (EXchange SpectroscopY) measurements were carried out with a 5 mm standard probe on both glass sphere systems (the crude and the sifted materials with dispersions of 30% and 18%, respectively) and the polystyrene material, using mixing times in the range 1.3 ms–2 s.

References

[1] W.S. Price, Pulsed-field gradient nuclear magnetic resonance as a tool for studying translational diffusion: Part1. Basic theory, Concepts Magn. Reson. 9 (1997) 299–335.

[2] P.T. Callaghan, Principle of Nuclear Magnetic Resonance Microscopy, Oxford Science Publications, New York, 1991.

[3] J. -F Kuntz, G. Trausch, P. Palmas, P. Mutzenhardt, D. Canet, Diffusive diffraction phenomenon in a porous polymer material observed by NMR using r-f field gradients, J. Chem. Phys. 126 (2007) 134904-1–134904-6.

[4] J.-F. Kuntz, P. Palmas, D. Canet, Diffusive diffraction measurements in porous media: effect of structural disorder and internal magnetic field gradients, J. Magn. Reson. 188 (2007) 322–329.

[5] P.P. Mitra, P.N. Sen, L.M. Schwartz, P. Le Doussal, Diffusion propagator as a probe of the structure of porous media, Phys. Rev. Lett. 68 (1992) 3555–3558.

[6] L. L Latour, R.L. Kleinberg, P.P. Mitra, C.H. Sotak, Pore size distributions and tortuosity in heterogeneous porous media, J. Magn. Reson. Ser. A 112 (1995) 83–91.

[7] J.G. Seland, M. Ottaviani, B. Holfskjold, A PFG-NMR study of restricted diffusion in heterogeneous polymer particles, J. Colloid Interface Sci. 239 (2001) 168–177.

[8] P.Z. Sun, J.G. Seland, D. Cory, Background gradient suppression in pulsed gradient stimulated echo measurements, J. Magn. Reson. 161 (2003) 168–173.

[9] R.L. Karlieck, I.J. Lowe, A modified pulsed gradient technique for measuring diffusion in the presence of large background gradient, J. Magn. Reson. 37 (1980) 75–91.

[10] R.M. Cotts, M.J.R. Hoch, T. Sun, J.T. Markert, Pulsed field gradient stimulated echo methods for improved NMR diffusion measurements in heterogeneous systems, J. Magn. Reson. 83 (1989) 252–266.

[11] L.L. Latour, P.P. Mitra, R.L. Kleinberg, C.H. Sotak, Time-dependent diffusion coefficient of fluids in porous media as a probe of surface-to-volume ratio, J. Magn. Reson. Ser. A 101 (1993) 342–346.

[12] M.D. Hürlimann, K.G. Helmer, L.L. Latour, C.H. Sotak, Restricted diffusion in sedimentary rocks. Determination of surface-area-to-volume ratio and surface relaxivity, J. Magn. Reson. Ser. A. 111 (1994) 169–178.

[13] R.L. Kleinberg, Pore size distributions, pore coupling, and transverse relaxation spectra of porous rocks, Magn. Reson. Imag. 12 (2) (1994) 271–274.

[14] L. Rijniers, L. Pel, H.P. Huininh, K. Kopinga, Pore size distribution from hydrogen and sodium NMR using the transverse relaxation at 4.7 T, Magn. Reson. Imag. 19 (3–4) (2001) 580.

[15] L. Venkataramaman, Y.Q. Song, M.D. Hürlimann, Solving Fredholm integrals of the first kind with tensor product structure in 2 and 2.5 dimensions, IEEE Trans. Signal. Process. 50 (2002) 1017–1026.

[16] B. Sun, K.-J. Dunn, Two-dimensional nuclear magnetic resonance petrophysics, Magn. Reson. Imag. 23 (2) (2005) 259–262.

[17] S. Godefroy, P.T. Callaghan, 2D relaxation/diffusion correlations in porous media, Magn. Reson. Imag. 21 (3–4) (2003) 381–383.

[18] A. Mutina, M.D. Hürlimann, NMR characterization of complex fluids by diffusion–relaxation distribution functions, Magn. Reson. Imag. 25 (4) (2007) 574.

[19] K.E. Washburn, P.T. Callaghan, Tracking pore to pore exchange using relaxation exchange spectroscopy, Phys. Rev. Lett. 97 (2006) 175502-1–175502-4.

[20] J. Jeener, B.H. Meier, P. Bachmann, R.R. Ernst, Investigation of exchange processes by 2D NMR spectroscopy, J. Chem. Phys. 71 (1979) 4546–4553.

[21] R.R. Ernst, G. Bodenhausen, A. Wokaun, Principles of Nuclear Magnetic Resonance in One and Two Dimensions, Oxford Science Publications, New York, 1987.

[22] K. Knagge, J.R. Smith, L.J. Smith, J. Buriak, D. Raftery, Analysis of porosity in porous silicon using hyperpolarized ^{129}Xe 2D exchange experiments, Sol. State Nuc. Magn. Reson. 29 (2006) 85–89.

[23] E.O. Stejskal, J.E. Tanner, Spin diffusion measurements: Spin echoes in the presence of a time-dependent field gradient, J. Chem. Phys. 42 (1965) 288–292.

[24] M.A. Delsuc, T.E. Malliavin, Maximum entropy processing of DOSY NMR spectra, Anal. Chem. 70 (1998) 2146–2148.